Hajjaj et al. EURASIP Journal on Wireless Communications and Networking (2015) 2015:56
DOI 10.1186/s13638-015-0293-6

EURASIP Journal on Wireless Communications and Networking
a SpringerOpen Journal

RESEARCH Open Access

Low-complexity WLMMSE channel estimator for MB-OFDM UWB systems

Moufida Hajjaj[1*], Walid Chainbi[2] and Ridha Bouallegue[3]

Abstract

Widely linear (WL) minimum mean square error (MMSE) channel estimation scheme have been proposed for multiband orthogonal frequency division multiplexing ultra-wideband (MB-OFDM UWB) systems dealing with non-circular signals. This WLMMSE channel estimation scheme provides significant performance gain, but it presents a high computational complexity compared with the linear one. In this paper, we derive an adaptive WLMMSE channel estimation scheme that significantly reduces the computational complexity. The complexity reduction is done in two stages. The first stage consists of a real evaluation of the WLMMSE channel estimator and the second stage follows with a reduced-rank filtering based on the singular value decomposition (SVD). Computational complexity evaluation shows that the proposed low-rank real-valued WLMMSE channel estimator has computation cost comparable with the linear MMSE. Additionally, simulations of the bit error rate (BER) performance show comparable performance with the WLMMSE channel estimator especially at high signal-to-noise ratio (SNR).

Keywords: Widely linear estimation; Computational complexity; Low rank; Real valued; MB-OFDM; UWB

1 Introduction

Over the past few years, ultra-wideband (UWB) has been promised as an efficient technology for future wireless short-range high data rate communication [1]. It has received great attention in both academia and industry for applications in wireless communications since 2002 when the Federal Communications Commission (FCC) of the USA reserved the frequency band between 3.1 and 10.6 GHz for indoor UWB applications. This decision has led to the introduction of Institute of Electrical and Electronic Engineering (IEEE) 802.15 high rate alternative physical layer (PHY) Task Group 3a for wireless personal area networks (WPAN). And ever since then, various researches on UWB systems have been conducted all over the world for the final high-speed WPAN standard. One of them, the multiband orthogonal frequency division multiplexing (MB-OFDM)-based UWB system has been proposed, by the Multiband OFDM Alliance (MBOA), for European Computer Manufacturers Association (ECMA)-368 standard to provide low power and high data rate transmission [2-4].

A collection of problems including channel measurements and modeling, channel estimation, and synchronization have been widely studied by researchers [5-10]. Clearly, all the performance improvement and capacity increase are based on accurate channel state information. Therefore, the most important component of MB-OFDM UWB system, represented by the block diagram of Figure 1, is that blue highlighted channel estimation and equalization component.

In the UWB literature, the channel estimation has mostly been studied for its effect on error rate performance and computational complexity [8-18]. For example, a minimum mean square error (MMSE) estimator has been proposed by Beek et al., and they have shown that it gives a performance gain over least square (LS) estimator [8]. Moreover, Li et al. have proposed a low-complexity channel estimator developed by first averaging the overlap-added (OLA) received preamble symbols within the same band and then applying time-domain least squares method followed by the discrete Fourier transform [9]. Also, a low-sampling-rate scheme, based on multiple observations generated by transmitting multiple pulses, for ultra-wideband channel estimation has been proposed in [12]. Furthermore, authors in [18] propose preamble-based improved channel estimation in the presence of both

* Correspondence: moufida.hajjaj@gmail.com
[1]National Engineering School of Tunis/Innov'COM Lab, University of El-Manar, El Manar 1, 1068 Tunis, Tunisia
Full list of author information is available at the end of the article

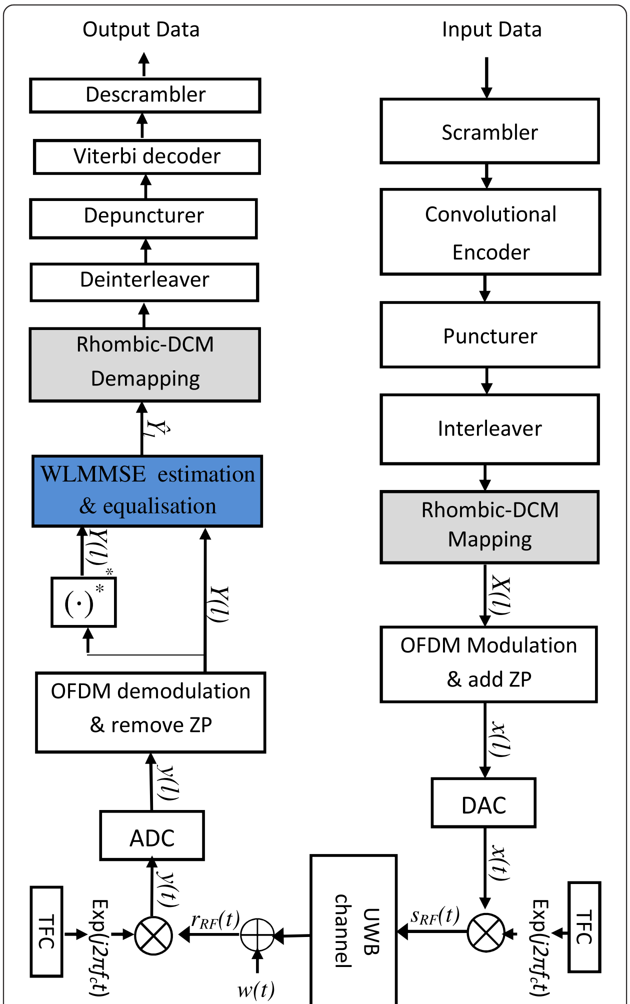

Figure 1 The structure of a multiband OFDM UWB. OFDM UWB, orthogonal frequency division multiplexing ultra-wideband.

multiple-access interference (MAI) and narrowband interference (NBI). The afore-mentioned estimators are applied for strictly linear systems.

Outside the UWB literature, there has been growing interest to widely linear (WL) processing which takes into account both the original values of the signal data as well as their conjugates. For example, Chevalier et al. have presented the widely linear mean square estimation with complex data [19,20]. They have shown that widely linear systems outperform significantly the strictly linear one. Also, Sterle has compared linear and widely linear MMSE transceivers for multiple input multiple output (MIMO) channels [21]. The results have shown that the widely linear MMSE transceiver provides considerable mean square error (MSE) and signal error rate (SER) gains over the linear one. Similarly, Cheng and Haardt have investigated the use of widely linear processing for MIMO systems employing filter bank multi-carrier/offset quadrature amplitude modulation (FBMC/OQAM) [22]. Moreover, the WL processing has been considered to channel estimation firstly in [23] for multi-carrier code division multiple access (MC-CDMA) systems and it has been shown via simulations that the asymptotic bias and the MSE are significantly reduced when WL processing is employed. Furthermore, the WL processing has been investigated to suppress inter-/intra-symbol interference, multiuser interference, and narrowband interference in a high data rate direct sequence ultra-wideband (DS-UWB) system [24]. The WL processing has shown that it outperforms the linear one. However, it has been shown that the WL processing presented a high computational cost [24-26].

Many studies (see, e.g., [24,27-38]) have shown that significant complexity reduction can be achieved by rank reduction techniques. Among these techniques, the eigenvalue decomposition (EVD) and its related singular value decomposition (SVD) techniques have had growing interest. For example, a reduced-rank maximum likelihood estimation (RRMLE) has been derived in [27] for the ML estimation of the regression matrix in terms of the data covariances and their Eigen elements. Also, Scharf and Van Veen have proposed low-rank detectors for gaussian random vectors, and they have shown that rank reduction can be performed with no loss in performance [28]. Novel reduced-rank scheme based on joint iterative optimization of adaptive filters with a low-complexity implementation using normalized least mean square (NLMS) algorithms has been proposed in [29]. The simulation results of the proposed scheme for CDMA interference suppression show a performance significantly better than existing schemes and close to the optimal full-rank MMSE. Moreover, Marzook et al. have proposed a novel channel estimation technique based on SVD technique for time division code division multiple access (TD-SCDMA) [30]. The results have shown that the proposed technique improves the performance of the TD-SCDMA system with low-rank processing and low computation complexity. Furthermore, channel estimation techniques based on SVD for reduced-rank MIMO systems have been proposed in [36]. It has been shown that the SVD-based estimation largely improves the system performance. In all these studies, it has been proved that the rank reduction techniques, especially SVD technique, give a best tradeoff between performance and complexity.

The aim of the paper is twofold. Firstly, based on complex-to-real transformation, we propose a real-valued WLMMSE channel estimator algorithm. Secondly, and based on SVD technique, we propose to reduce the rank of the obtained real-valued WLMMSE channel estimator.

The rest of the paper is organized as follows. MB-OFDM UWB system model describes the system model. The structure of the proposed low-rank real-valued widely linear minimum mean square error (Lr-RWLMMSE) channel estimator is presented in channel estimation. Computational complexity evaluation is dedicated to the computational complexity evaluation of the conventional and proposed schemes. Performance evaluations provide the performance evaluations. Finally, some concluding comments are given in 'Conclusions'.

2 MB-OFDM UWB system model

Multiband OFDM (MB-OFDM) is the main solution considered for high rate UWB transmission. Firstly, it was proposed by A. Batra et al. from Texas Instruments for the IEEE 802.15.3a task group [3]. Secondly, it was introduced by the MBOA consortium as their global UWB standard [4]. According to this standard, the available spectrum (3.1 – 10.6 GHz) is divided into 14 sub-bands. Each sub-band of 528 MHz offers 480 Mbit/s. In order to introduce multiple accessing capabilities and to exploit the inherent frequency diversity, each OFDM symbol obtained from a 128-point inverse fast Fourier transform (IFFT), is transmitted on a different sub-band as dictated by a time-frequency code (TFC), shown in Figure 2, that leads to band hopping [4]. The architectures of the transmitter and the receiver of a MB-OFDM UWB system, based on the specifications of ECMA-368 standard, are shown in Figure 1. The modified blocks are those highlighted. These blocks are mainly the rhombic-dual carrier modulation (DCM) mapping at the transmitter and the rhombic-DCM demapping at the receiver proposed by Hajjaj et al. (unpublished work) for MB-OFDM UWB systems. In addition, low-rank real-valued WLMMSE channel estimation and equalization is applied. All MB-OFDM UWB system parameters are detailed in Table 1.

At the baseband transmitter, the bits from information sources are first scrambled into a pseudo random sequence. The resulting scrambled sequence is then encoded using convolutional encoder of rate $R = 1/3$ and constraint length $K = 7$, interleaved via bit interleaver and converted into the l^{th} OFDM symbol of $N_D = 100$ tones. The N_D energy-carrying tones are modulated using rhombic-DCM. Then, a total of $N_P = 12$ pilot tones, $N_G = 10$ guard tones and 6 null tones are inserted into the OFDM symbol. An IFFT is used to transform the block of N_{IFFT} ($N_{IFFT} = N_D + N_P + N_G + 6$ nulls) tones into time-domain. The duration for the OFDM symbol is $T_{IFFT} = 242.42$ ns. Then, a zero padding sequence of length $N_{ZP} = 32$ and duration $T_{ZP} = 60.61$ ns is added to the resulting time-domain OFDM symbol, to eliminate the intersymbol interference (ISI) caused by the multipath propagation, and a guard interval of length 5 and duration $T_{GI} = 9.47$ ns is added to the end of the OFDM symbol, to ensure the frequency hopping. Thus, each transmitted OFDM symbol has a duration $T_S = T_{IFFT} + T_{ZP} + T_{GI} = 312.5$ ns and includes $N_S = N_{IFFT} + N_{ZP} + 5 = 165$ subcarriers.

The useful discrete-time OFDM signal model is defined by:

$$x(l,n) = \frac{1}{\sqrt{N_{\mathrm{IFFT}}}}\left[\sum_{k=0}^{N_D-1} D(l,k)e^{\frac{j2\pi q_D(k)n}{N_{\mathrm{IFFT}}}} + \sum_{k=0}^{N_P-1} P(l,k)e^{\frac{j2\pi q_P(k)n}{N_{\mathrm{IFFT}}}} + \sum_{k=0}^{N_G-1} G(l,k)e^{\frac{j2\pi q_G(k)n}{N_{\mathrm{IFFT}}}}\right] \quad (1)$$

where $n = 0,\ldots, N_{IFFT} - 1$, D, P and G are the k^{th} data, pilot, and guard subcarriers of the l^{th} OFDM symbol, respectively, and the functions q_D, q_P, and q_G define a mapping functions for data, pilot, and guard subcarriers, respectively.

The baseband of the receiver, in general, consists of similar blocks of the baseband in the transmitter but in the reverse order [2].

The RF-transmitted signal is obtained by converting the baseband signal into continuous-time waveforms via a digital-to-analog converter (DAC) and then up-converting it to the appropriate center frequency, as:

$$s_{\mathrm{RF}}(t) = \mathrm{Re}\left\{\sum_{l=0}^{N_{\mathrm{sym}}-1} x(t-lT_S)e^{j2\pi f_c(q(l))t}\right\} \quad (2)$$

where Re(·) represents the real part of the signal, Nsym is the number of symbols, $f_c(m)$ is the center frequency for the m^{th} frequency band, $q(l)$ is a function that maps

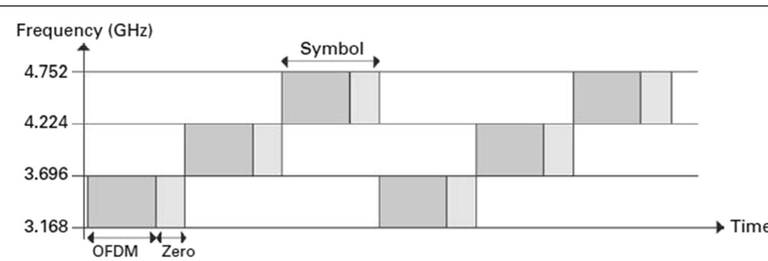

Figure 2 Time-frequency coding for the MB-OFDM system using the first three bands with a TFC of {1, 2, 3, 1, 2, 3} [39]. OFDM, orthogonal frequency division multiplexing.

Table 1 MB-OFDM UWB system parameters

Parameter	Value
N_{IFFT}	128
Zero padding (ZP)	32
N_{D}: Number of data subcarriers	100
N_{P}: Number of pilot subcarriers	12
N_{G}: Number of guard subcarriers	10
ΔF: Subcarrier frequency spacing	4.125 MHz
T_{u}: IFFT/FFT period	242.42 ns
T_{ZP}: Zero padding duration	60.61 ns
T_{GI}: Guard interval duration	9.47 ns
T_{S}: Total duration of an OFDM symbol	312.5 ns
Constellation	Rhombic-DCM
Data rate	480 Mbps
B_{w}: Bandwidth	528 MHz

OFDM, orthogonal frequency division multiplexing; DCM, dual carrier modulation; IFFT, inverse fast Fourier transform; MB-OFDM UWB, multiband orthogonal frequency division multiplexing ultra-wideband.

the l^{th} symbol to the appropriate frequency band, and *x(t)* is the complex baseband signal representation for the l^{th} symbol. *x(t)* must satisfy the following property: $x(t) = 0$ for $t \notin [0, \mathrm{T_S}]$.

The radiated signal $S_{\mathrm{RF}}(t)$ is transmitted over the UWB channel proposed for the IEEE 802.15.3a standard [40]. The impulse response of the multipath UWB channel model is described as:

$$h_i(t) = \chi_i \sum_{l=0}^{L} \sum_{k=0}^{K} \alpha_{k,l}^{i} \delta\left(t - T_l^i - \tau_{k,l}^{i}\right) \tag{3}$$

where $\left\{\alpha_{k,l}^{i}\right\}$ and $\left\{\tau_{k,l}^{i}\right\}$ are the gain and the delay of the k^{th} multipath component relative to the l^{th} cluster arrival time $\left(T_l^i\right)$, respectively, $\{\chi_i\}$ is the log-normal shadowing of the i^{th} channel realization.

The IEEE 802.15.3a task group also defined four different configurations (CM1, CM2, CM3, and CM4) identified by the propagation scenarios line of sight (LOS) and non-line of sight (NLOS), and the distance between the transmitting and receiving antennas. The main characteristics of the UWB channel models are listed in Table 2.

Table 2 UWB channel models characteristics

	CM1	CM2	CM3	CM4
Mean excess delay (ns)	5.05	10.38	14.18	30
Delay spread (ns)	5.28	8.03	14.28	25
Distance (m)	0 to 4	0 to 4	4 to 10	10
LOS/NLOS	LOS	NLOS	NLOS	NLOS

LOS, line of sight; NLOS, non-line of sight; UWB, ultra-wideband.

The discrete-time UWB channel is modeled as a N_h-tap finite-impulse-response (FIR) filter whose channel frequency response (CFR) of the l^{th} OFDM symbol on its corresponding sub-band is given by:

$$H(l) = [H(l,0),\ H(l,1), \ldots, H(l, N_{\mathrm{IFFT}}-1)]^T \tag{4}$$

where $(\cdot)^T$ denotes the transposition operation.

At the receiver side, the received signal $r_{\mathrm{RF}}(t)$, which is the sum of the output of the channel and additive white Gaussian noise (AWGN) $w(t)$, is first filtered via band-pass filter and down-converted to baseband, and then the zero padding is removed using OLA method [41]. Then, the unitary fast Fourier transform (FFT) is applied to transform the discrete combined signal into frequency domain as:

$$Y(1) = X(l)H(l) + W(l) \tag{5}$$

where $X(l) = \mathrm{diag}\{X(l,\ 0),\ X(l,\ 1),\ \ldots,\ X(l,\ N_{\mathrm{IFFT}} - 1)\}$ represents the transmitted data, $Y(l) = [Y(l, 0), Y(l, 1), \ldots, Y(l, N_{\mathrm{IFFT}} - 1)]^T$ denotes the received data, and $W(l) = [W(l,0),\ W(l,1),\ \ldots,\ W(l, N_{IFFT}-1)]^T$ indicates the additive noise component, of the l^{th} OFDM symbol.

For the sake of simplicity, we refer, in this paper, to $Y(l)$, $X(l)$, $H(l)$, and $W(l)$ as Y, X, H, and W, respectively.

Wiener filter (WF) based on LMMSE criterion, employing the second-order statistics of the channel conditions, is considered for channel estimation [8]. However, since the proposed MB-OFDM UWB system is dealing with non-circular signals, it requires widely linear processing to take into account all the second-order statistics of the channel conditions and the received signal. Therefore, the received signal, in the frequency domain, is augmented with its conjugate as:

$$\begin{aligned} \underline{Y} &= \begin{bmatrix} Y \\ Y^* \end{bmatrix} = \begin{bmatrix} XH \\ X^*H^* \end{bmatrix} + \begin{bmatrix} W \\ W^* \end{bmatrix} \\ &= \begin{bmatrix} X & 0 \\ 0 & X^* \end{bmatrix} \begin{bmatrix} H \\ H^* \end{bmatrix} + \begin{bmatrix} W \\ W^* \end{bmatrix} \\ &= \underline{XH} + \underline{W} \end{aligned} \tag{6}$$

3 Channel estimation

The MB-OFDM UWB systems employ frame-based transmission. As shown in Figure 3, each MB-OFDM UWB frame, which is referred to PPDU (PLCP protocol data unit), is composed of three components: the PLCP (Physical Layer Convergence Protocol) preamble, the PLCP header, and the PSDU (PLCP service data unit) [3]. The PLCP preamble consists of three distinct portions: packet synchronization sequence, frame synchronization sequence, and the channel estimation sequence. The latter portion is used to estimate the channel frequency response. The channel estimation sequence is followed by the PLCP Header which contains the data rate, the data length, the

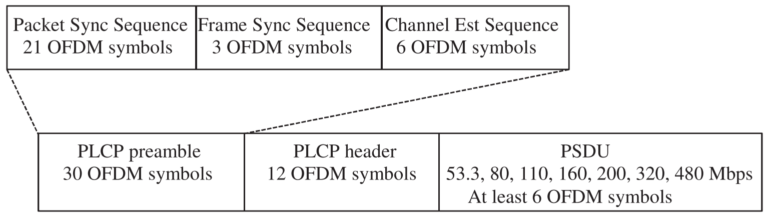

Figure 3 PLCP protocol data unit (PPDU) structure.

transport mode, the preamble type, and the MAC Header. The last component of the PPDU is the PSDU, which contains the actual information data (coming from higher layers).

We focus in this section on channel estimation for MB-OFDM UWB systems. There are two main methods: the first is based on the channel estimation sequence (CES) of the PLCP preamble and the second is based on pilot signals insertion into each OFDM symbol. Here, even assuming that the UWB channel is invariant over the transmission period of an OFDM frame, the channel estimation can be performed using the channel training sequence.

In the end of the MB-OFDM UWB system model, we have shown the relation between the augmented output $\underline{Y}$ and the augmented transmitted symbol $\underline{X}$ as:

$$\underline{Y} = \underline{X}\,\underline{H} + \underline{W} \tag{7}$$

This relation can be equally written for the N $(N = 112)$ CSES data subcarriers of a single training OFDM symbol as:

$$\breve{\underline{Y}} = \breve{\underline{X}}\,\breve{\underline{H}} + \breve{\underline{W}} \tag{8}$$

where $\breve{\underline{X}}$ is $2\,N \times 2\,N$ diagonal matrix with diagonal entries the N nonzero transmitted data augmented with its conjugate, $\breve{\underline{Y}}$, $\breve{\underline{H}}$ and $\breve{\underline{W}}$ are $2\,N \times 1$ related sub-blocks of $\underline{Y}$, $\underline{H}$ and $\underline{W}$, respectively.

3.1 Augmented LS estimator

Let $\widehat{\underline{H}}$ be the estimate of $\breve{\underline{H}}$. The expression of augmented LS estimation is:

$$\widehat{\underline{H}}_{LS} = \breve{\underline{X}}^{-1}\breve{\underline{Y}} \tag{9}$$

which minimizes $\left(\breve{\underline{Y}} - \breve{\underline{X}}\,\breve{\underline{H}}\right)^H \left(\breve{\underline{Y}} - \breve{\underline{X}}\,\breve{\underline{H}}\right)$

3.2 WLMMSE estimator

We denote the widely linear estimator of the augmented transfer function of channel $\breve{\underline{H}}$ by:

$$\widehat{\underline{H}}_{\text{WLMMSE}} = \breve{A}\,\breve{\underline{Y}} \tag{10}$$

Based on the orthogonality principle for linear estimation $E\left[\left(\widehat{\underline{H}}_{\text{WLMMSE}} - \breve{\underline{H}}\right)\breve{\underline{Y}}^H\right] = 0$ [42], the optimal $\breve{A}$ is given by:

$$\breve{A} = E\left[\breve{\underline{H}}\,\breve{\underline{Y}}^H\right]\left(E\left[\breve{\underline{Y}}\,\breve{\underline{Y}}^H\right]\right)^{-1} = C_{\breve{\underline{H}}\breve{\underline{Y}}}C^{-1}_{\breve{\underline{Y}}\breve{\underline{Y}}} \tag{11}$$

Hence, the WLMMSE estimator of $\breve{\underline{H}}$ can be written as:

$$\widehat{\underline{H}}_{\text{WLMMSE}} = C_{\breve{\underline{H}}\breve{\underline{Y}}}C^{-1}_{\breve{\underline{Y}}\breve{\underline{Y}}}\breve{\underline{Y}} \tag{12}$$

where the augmented auto-covariance matrix of $\breve{\underline{Y}}$ is given by:

$$\underline{C}_{\breve{Y}\breve{Y}} = \begin{bmatrix} \breve{X}C_{\breve{H}\breve{H}}\breve{X}^* + \sigma^2_{\breve{W}} & \breve{X}\tilde{C}_{\breve{H}\breve{H}}\breve{X} \\ \breve{X}^*\tilde{C}^*_{\breve{H}\breve{H}}\breve{X}^* & \breve{X}^*C^*_{\breve{H}\breve{H}}\breve{X} + \sigma^2_{\breve{W}} \end{bmatrix} \tag{13}$$

and the augmented cross-covariance matrix is defined as:

$$\underline{C}_{\breve{H}\breve{Y}} = \begin{bmatrix} C_{\breve{H}\breve{H}}\breve{X}^* & \tilde{C}_{\breve{H}\breve{H}}\breve{X} \\ \tilde{C}^*_{\breve{H}\breve{H}}\breve{X}^* & C^*_{\breve{H}\breve{H}}\breve{X} \end{bmatrix} \tag{14}$$

In strictly linear case, the LMMSE estimator is given by:

$$\begin{aligned} \widehat{H}_{\text{LMMSE}} &= C_{\breve{H}\breve{Y}}C^{-1}_{\breve{Y}\breve{Y}}\breve{Y} \\ &= C_{\breve{H}\breve{H}}\left(C_{\breve{H}\breve{H}} + \sigma^2_{\breve{W}}\left(\breve{X}\,\breve{X}^*\right)^{-1}\right)^{-1}\widehat{H}_{LS} \end{aligned} \tag{15}$$

3.3 Low-rank real-valued WLMMSE estimator

We denote by H_R, X_R, W_R, and Y_R the real composite representation of $\breve{H}, \breve{X}, \breve{W}$, and $\breve{Y}$, respectively:

$$H_R = \begin{bmatrix} H_r \\ H_i \end{bmatrix} \tag{16}$$

where H_r and H_i are the real and imaginary vectors of $\breve{H}$

$$X_R = \begin{bmatrix} X_r & -X_i \\ X_i & X_r \end{bmatrix} \tag{17}$$

where X_r and X_i are the real and imaginary matrices of $\breve{X}$

$$W_R = \begin{bmatrix} W_r \\ W_i \end{bmatrix} \tag{18}$$

where W_r and W_i are the real and imaginary vectors of $\breve{W}$

$$Y_R = \begin{bmatrix} Y_r \\ Y_i \end{bmatrix} \tag{19}$$

where Y_r and Y_i are the real and imaginary vectors of $\breve{Y}$.

From (16) and (17):

$$\breve{X}\breve{H} = X_r H_r - X_i H_i + j(X_r H_i + X_i H_r) \tag{20}$$

Then,

$$\begin{aligned} Y_R = \begin{bmatrix} Y_r \\ Y_i \end{bmatrix} &= \begin{bmatrix} X_r H_r - X_i H_i \\ X_r H_i + X_i H_r \end{bmatrix} + \begin{bmatrix} W_r \\ W_i \end{bmatrix} \\ &= \begin{bmatrix} X_r & -X_i \\ X_i & X_r \end{bmatrix} \begin{bmatrix} H_r \\ H_i \end{bmatrix} + \begin{bmatrix} W_r \\ W_i \end{bmatrix} \end{aligned} \tag{21}$$

The linear-to-complex transformation gives the following relations

- The relation between the augmented vector $\underline{\breve{Y}}$ and the real vector Y_R can be described by: $\underline{\breve{Y}} = TY_R$ where $T = \begin{bmatrix} I & jI \\ I & -jI \end{bmatrix}$ is unitary up to a factor of 2: $TT^H = T^H T = 2I$, and I is the identity matrix.
- The relation between the augmented vector $\underline{\breve{W}}$ and the real vector W_R can be described by $\underline{\breve{W}} = TW_R$.
- The relation between the augmented vector $\underline{\breve{H}}$ and the real vector H_R can be described by $\underline{\breve{H}} = TH_R$.

We assume that $\breve{H}$ and $\breve{W}$ are uncorrelated as in all stochastic filtering applications, i.e., $\breve{H}\breve{W}^H = \breve{W}\breve{H}^H = 0$.

Then, the augmented auto-covariance matrix of $\breve{Y}$ can be expressed as:

$$\begin{aligned} C_{\underline{\breve{Y}}\,\underline{\breve{Y}}} &= E\left[\underline{\breve{Y}}\,\underline{\breve{Y}}^H\right] \\ &= E\left[(TY_R)(TY_R)^H\right] \\ &= E\left[TY_R Y_R^H T^H\right] \\ &= TE\left[Y_R Y_R^H\right] T^H \\ &= TR_{Y_R Y_R} T^H \end{aligned} \tag{22}$$

where $R_{Y_R Y_R}$ is the auto-correlation matrix of Y_R.

$$\begin{aligned} R_{Y_R Y_R} &= E\left[\left(\begin{bmatrix} X_r & -X_i \\ X_i & X_r \end{bmatrix}\begin{bmatrix} H_r \\ H_i \end{bmatrix} + \begin{bmatrix} W_r \\ W_i \end{bmatrix}\right) \times \left(\begin{bmatrix} X_r & -X_i \\ X_i & X_r \end{bmatrix}\begin{bmatrix} H_r \\ H_i \end{bmatrix} + \begin{bmatrix} W_r \\ W_i \end{bmatrix}\right)^H\right] \\ &= E\left(\begin{bmatrix} X_r & -X_i \\ X_i & X_r \end{bmatrix}\begin{bmatrix} H_r \\ H_i \end{bmatrix}\begin{bmatrix} H_r \\ H_i \end{bmatrix}^H\begin{bmatrix} X_r & -X_i \\ X_i & X_r \end{bmatrix}^H\right) \\ &\quad + E\left(\begin{bmatrix} W_r \\ W_i \end{bmatrix}\begin{bmatrix} W_r \\ W_i \end{bmatrix}^H\right) + E\left(\begin{bmatrix} X_r & -X_i \\ X_i & X_r \end{bmatrix}\begin{bmatrix} H_r \\ H_i \end{bmatrix}\begin{bmatrix} W_r \\ W_i \end{bmatrix}^H\right) \\ &\quad + E\left(\begin{bmatrix} W_r \\ W_i \end{bmatrix}\begin{bmatrix} H_r \\ H_i \end{bmatrix}^H\begin{bmatrix} X_r & -X_i \\ X_i & X_r \end{bmatrix}^H\right) \\ &= \begin{bmatrix} X_r & -X_i \\ X_i & X_r \end{bmatrix}\underbrace{E\left(\begin{bmatrix} H_r \\ H_i \end{bmatrix}\begin{bmatrix} H_r \\ H_i \end{bmatrix}^H\right)}_{R_{H_R H_R}}\begin{bmatrix} X_r & -X_i \\ X_i & X_r \end{bmatrix}^H \\ &\quad + E\left(\begin{bmatrix} W_r \\ W_i \end{bmatrix}\begin{bmatrix} W_r \\ W_i \end{bmatrix}^H\right) + \begin{bmatrix} X_r & -X_i \\ X_i & X_r \end{bmatrix}\underbrace{E\left(\begin{bmatrix} H_r \\ H_i \end{bmatrix}\begin{bmatrix} W_r \\ W_i \end{bmatrix}^H\right)}_{0} \\ &\quad + \underbrace{E\left(\begin{bmatrix} W_r \\ W_i \end{bmatrix}\begin{bmatrix} H_r \\ H_i \end{bmatrix}^H\right)}_{0}\begin{bmatrix} X_r & -X_i \\ X_i & X_r \end{bmatrix}^H \end{aligned} \tag{23}$$

$$\begin{aligned} E\left(\begin{bmatrix} W_r \\ W_i \end{bmatrix}\begin{bmatrix} W_r \\ W_i \end{bmatrix}^H\right) &= E\left(\left(T^{-1}\underline{\breve{W}}\right)\left(T^{-1}\underline{\breve{W}}\right)^H\right) \\ &= E\left(T^{-1}\underline{\breve{W}}\,\underline{\breve{W}}^H\right) \\ &= T^{-1}E\left(\underline{\breve{W}}\,\underline{\breve{W}}^H\right)\left(T^H\right)^{-1} \\ &= T^{-1}\sigma^2_{\underline{\breve{W}}}\left(T^H\right)^{-1} \\ &= \sigma^2_{\underline{\breve{W}}}\left(TT^H\right)^{-1} \\ &= 2\sigma^2_{\underline{\breve{W}}} I \end{aligned} \tag{24}$$

Then,

$$R_{Y_R Y_R} = X_R R_{H_R H_R} X_R^H + 2\sigma^2_{\underline{\breve{W}}} I \tag{25}$$

where $R_{H_R H_R}$ is the auto-correlation matrix of H_R.

The augmented cross-covariance matrix can be determined as:

$$\begin{aligned} C_{\underline{\breve{H}}\,\underline{\breve{Y}}} &= E\left[\underline{\breve{H}}\,\underline{\breve{Y}}^H\right] \\ &= E\left[(TH_R)(TY_R)^H\right] \\ &= E\left[TH_R Y_R^H T^H\right] \\ &= TE\left[H_R Y_R^H\right] T^H \\ &= TR_{H_R Y_R} T^H \end{aligned} \tag{26}$$

where

$$
\begin{aligned}
R_{H_R Y_R} &= E\left[\left(\begin{bmatrix} H_r \\ H_i \end{bmatrix}\right)\left(\begin{bmatrix} X_r & -X_i \\ X_i & X_r \end{bmatrix}\begin{bmatrix} H_r \\ H_i \end{bmatrix} + \begin{bmatrix} W_r \\ W_i \end{bmatrix}\right)^H\right] \\
&= E\left[\left(\begin{bmatrix} H_r \\ H_i \end{bmatrix}\begin{bmatrix} H_r \\ H_i \end{bmatrix}^H \begin{bmatrix} X_r & -X_i \\ X_i & X_r \end{bmatrix}^H\right)\right] \\
&\quad + \underbrace{E\left(\begin{bmatrix} H_r \\ H_i \end{bmatrix}\begin{bmatrix} W_r \\ W_i \end{bmatrix}^H\right)}_{0} \\
&= \underbrace{E\left(\begin{bmatrix} H_r \\ H_i \end{bmatrix}\begin{bmatrix} H_r \\ H_i \end{bmatrix}^H\right)}_{RH_RH_R}\begin{bmatrix} X_r & -X_i \\ X_i & X_r \end{bmatrix}^H \\
&= R_{H_R H_R} X_R^H
\end{aligned}
\tag{27}
$$

By inserting the expression of $\underline{C}_{\underline{\breve{H}}\,\underline{\breve{Y}}}$, $\underline{C}_{\underline{\breve{Y}}\,\underline{\breve{Y}}}$, and $\underline{\breve{Y}}$ into (12), the resulting real-valued WLMMSE (RWLMMSE) estimator of $\underline{H}$ is denoted by:

$$
\begin{aligned}
\widehat{\underline{H}}_{\text{RWLMMSE}} &= \left(TR_{H_R Y_R}T^H\right)\left(TR_{Y_R Y_R}T^H\right)^{-1}\left(TY_R\right) \\
&= TR_{H_R Y_R}T^H\left(T^H\right)^{-1}R_{Y_R Y_R}^{-1}T^{-1}TY_R \\
&= TR_{H_R Y_R}R_{Y_R Y_R}^{-1}Y_R \\
&= TR_{H_R H_R}X_R^H\left(X_R R_{H_R H_R}X_R^H + 2\sigma_{\underline{W}}^2 I\right)^{-1}Y_R
\end{aligned}
\tag{28}
$$

The LS estimator of $\underline{\breve{H}}$ is:

$$
\widehat{\underline{H}}_{LS} = \underline{X}^{-1}\underline{\breve{Y}} \Leftrightarrow \underline{\breve{Y}} = \underline{\breve{X}}\,\widehat{\underline{H}}_{LS} \Leftrightarrow Y_R = X_R \widehat{H}_{LS_R} \tag{29}
$$

where $H_{LS_R} = \begin{pmatrix} H_{LS_r} \\ H_{LS_i} \end{pmatrix}$, and H_{LS_r} and H_{LS_i} are the real and imaginary vectors of $\breve{H}_{LS}$.

Then,

$$
\begin{aligned}
\widehat{\underline{H}}_{\text{RWLMMSE}} &= TR_{H_R H_R}X_R^H\left(X_R R_{H_R H_R}X_R^H + 2\sigma_{\underline{W}}^2 I\right)^{-1}X_R\widehat{H}_{LS_R} \\
&= TR_{H_R H_R}X_R^H X_R\left(X_R R_{H_R H_R}X_R^H + 2\sigma_{\underline{W}}^2 I\right)^{-1}\widehat{H}_{LS_R} \\
&= TR_{H_R H_R}\left(R_{H_R H_R} + 2\sigma_{\underline{W}}^2\left(X_R X_R^H\right)^{-1}\right)^{-1}\widehat{H}_{LS_R} \\
&= TR_{H_R H_R}\left(R_{H_R H_R} + \xi I\right)^{-1}\widehat{H}_{LS_R}
\end{aligned}
\tag{30}
$$

where

$$
\xi = \frac{2\sigma_{W_R}^2}{\sigma_{X_R}^2} \tag{31}
$$

To further reduce the computational complexity, we adopt the low-rank approximation technique based on SVD [35]. The SVD of $R_{H_R H_R}$ is denoted by $R_{H_R H_R} = U\Lambda U^H$, where U is a matrix with orthonormal columns $u_0, u_1, \ldots, u_{2N-1}$ and Λ is a diagonal matrix, containing the singular values $\lambda_0 \geq \lambda_1 \geq \ldots \geq \lambda_{2N-1} \geq 0$ on its diagonal. Since some singular values of the matrix Λ are negligible, by selecting r significant singular values, we can obtain optimal rank r channel estimator.

The proposed rank r channel estimator is given by:

$$
\widehat{\underline{H}}_{\text{Lr-RWLMMSE}} = TU\begin{pmatrix} \Delta_r & 0 \\ 0 & 0 \end{pmatrix}U^H\widehat{H}_{LS_R} \tag{32}
$$

where Δ_r is a diagonal matrix containing the values:

$$
\delta_k = \frac{\lambda_k}{\lambda_k + \xi}, k = 0, 1, \ldots, r-1 \tag{33}
$$

4 Computational complexity evaluation

In this section, we analyze the performance of our proposed estimator in terms of computational complexity. It is shown that the multiplication of two $N \times N$ complex matrixes requires $3N^3 + 2N^2$ real additions and $4N^3$ real multiplications [43].

➢ The calculation of $\widehat{\underline{H}}_{\text{WLMMSE}}$ requires:

- $12N^3 + 8N^2$ real additions and $12N^3$ real multiplications to calculate $\underline{C}_{\breve{H}\breve{Y}}$,
- $24N^3 + 20N^2$ real additions and $24N^3$ real multiplications to calculate $\underline{C}_{\breve{Y}\breve{Y}}$,
- $8N^3$ operations to calculate the inverse of $\underline{C}_{\breve{Y}\breve{Y}}$,
- $48N^3 + 8N^2$ operations to calculate the product of $\underline{C}_{\breve{H}\breve{Y}}$ by $\underline{C}_{\breve{Y}\breve{Y}}^{-1}$,
- and $64N^2$ operations to calculate the product of $\underline{C}_{\breve{H}\breve{Y}}\underline{C}_{\breve{Y}\breve{Y}}^{-1}$ by $\underline{\breve{Y}}$.

Then, the computational complexity of $\widehat{\underline{H}}_{\text{WLMMSE}}$ is given by:

$$
\begin{aligned}
O\left(\widehat{\underline{H}}_{\text{WLMMSE}}\right) &= 12N^3 + 8N^2 + 12N^3 + 24N^3 + 20N^2 \\
&\quad + 24N^3 + 8N^2 + 48N^3 + 8N^2 \\
&\quad + 64N^2 \\
&= 120N^3 + 108N^2
\end{aligned}
\tag{34}
$$

➢ The calculation of $\hat{H}_{\text{LMMSE}}$ requires:

- $3N^3 + 2N^2$ real additions and $3N^3$ real multiplications to calculate $C_{\breve{H}\breve{Y}}$,
- $6N^3 + 5N^2$ real additions and $6N^3$ real multiplications to calculate $C_{\breve{Y}\breve{Y}}$,
- N^3 operations to calculate the inverse of $C_{\breve{Y}\breve{Y}}$,
- $6N^3 + 3N^2$ operations to calculate the product of $C_{\breve{H}\breve{Y}}$ by $C_{\breve{Y}\breve{Y}}^{-1}$,
- and $8N^2$ operations to calculate the product of $C_{\breve{H}\breve{Y}}C_{\breve{Y}\breve{Y}}^{-1}$ by $\breve{Y}$.

Then, the computational complexity of $\hat{H}_{\mathrm{LMMSE}}$ is given by:

$$O\left(\hat{H}_{\mathrm{LMMSE}}\right) = 3N^3 + 2N^2 + 3N^3 + 6N^3 + 5N^2 + 6N^3 + N^3 + 6N^3 + 3N^2 + 8N^2 = 25N^3 + 18N^2 \tag{35}$$

Therefore, the computational complexity of WLMMSE estimator requires about five times more operations than the LMMSE estimator.

➢ The calculation of $\underline{\hat{H}}_{\mathrm{RWLMMSE}}$ requires:

- $8N^3$ operations to calculate the product of T by $R_{H_R H_R}$,
- $4N^2$ operations to calculate the addition of $R_{H_R H_R}$ and ξI,
- $8N^3$ operations to calculate the inverse of $(R_{H_R H_R} + \xi I)$,
- $8N^3$ operations to calculate the product of $TR_{H_R H_R}$ by $(R_{H_R H_R} + \xi I)^{-1}$,
- and $4N^2$ operations to calculate the product of $TR_{H_R H_R}(R_{H_R H_R} + \xi I)^{-1}$ by $\hat{H}_{LS_R}$.

Then, the computational complexity of $\underline{\hat{H}}_{\mathrm{RWLMMSE}}$ is given by:

$$O\left(\underline{\hat{H}}_{\mathrm{RWLMMSE}}\right) = 8N^3 + 4N^2 + 8N^3 + 8N^3 + 4N^2 = 24N^3 + 8N^2 \tag{36}$$

➢ The calculation of $\underline{\hat{H}}_{\mathrm{Lr-RWLMMSE}}$ requires:

- $4N^2r + 2Nr$ operations to calculate $U\begin{pmatrix} \Delta_r & 0 \\ 0 & 0 \end{pmatrix}U^H$,
- $8N^3$ operations to calculate the product of T by $U\begin{pmatrix} \Delta_r & 0 \\ 0 & 0 \end{pmatrix}U^H$,
- and $4N^2$ operations to calculate the product of $TU\begin{pmatrix} \Delta_r & 0 \\ 0 & 0 \end{pmatrix}U^H$ by $\hat{H}_{LS_R}$.

Then, the computational complexity of $\underline{\hat{H}}_{\mathrm{Lr-RWLMMSE}}$ is given by:

$$O\left(\underline{\hat{H}}_{\mathrm{Lr\text{-}RWLMMSE}}\right) = 8N^3 + 4N^2r + 4N^2 + 2Nr \tag{37}$$

Thus, the computational complexity of $\underline{\hat{H}}_{\mathrm{RWLMMSE}}$ requires a total of $24N^3 + 8N^2$ operations, which is about 5 times less than that of $\underline{\hat{H}}_{\mathrm{WLMMSE}}$ and slightly less than that of $\hat{H}_{\mathrm{LMMSE}}$. Consequently, the real-valued WLMMSE channel estimator reduces the computational complexity by 80% and accomplishes a computational complexity comparable with that of LMMSE channel estimator. Furthermore, by applying the low-rank Wiener filter technique, the complexity of $\underline{\hat{H}}_{\mathrm{Lr\text{-}RWLMMSE}}$ is significantly reduced mainly for small values of r.

5 Performance evaluations

In this section, we compare the bit error rate (BER) of the proposed low-rank RWLMMSE channel estimator with that of WLMMSE channel estimator. The MB-OFDM UWB system parameters are summarized in Table 1. In our simulations, we adopt the CM1 and CM2 UWB channel models of the standard IEEE 802.15.3a.

In Figures 4 and 5, the BER performance of the proposed channel estimator for MB-OFDM UWB system for various values of rank r are evaluated in terms of signal-to-noise ratio (SNR) in CM1 and CM2, respectively. The used modulation is the rhombic-DCM with a rhombic deformation coefficient $\varepsilon = 0.5$. In these figures, the legends WLMMSE, Lr-RWLMMSE ($r = 16$), Lr-RWLMMSE ($r = 32$), and Lr-RWLMMSE ($r = 64$) present the estimators based on WLMMSE, Lr-RWLMMSE with rank $r = 16$, Lr-RWLMMSE with rank $r = 32$, and Lr-RWLMMSE with rank $r = 64$, respectively. In both figures, it is observed that the performance of the Lr-RWLMMSE estimator is comparable with that of WLMMSE at low SNR and slightly under the

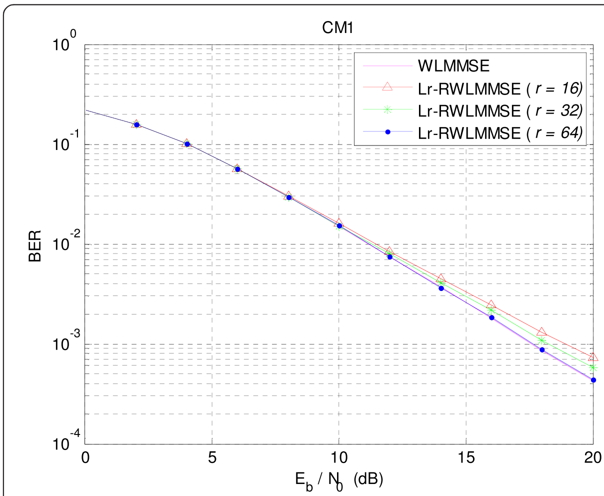

Figure 4 BER vs. SNR for WLMMSE and Lr-RWLMMSE estimators over CM1 channel model. BER, bit error rate; WLMMSE, widely linear minimum mean square error; Lr-RWLMMSE, low-rank real-valued widely linear minimum mean square error.

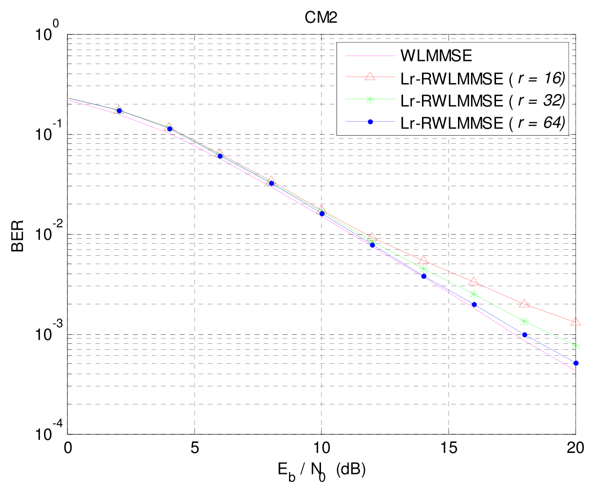

Figure 5 BER vs. SNR for WLMMSE and Lr-RWLMMSE estimators over CM2 channel model. BER, bit error rate; WLMMSE, widely linear minimum mean square error; Lr-RWLMMSE, low-rank real-valued widely linear minimum mean square error.

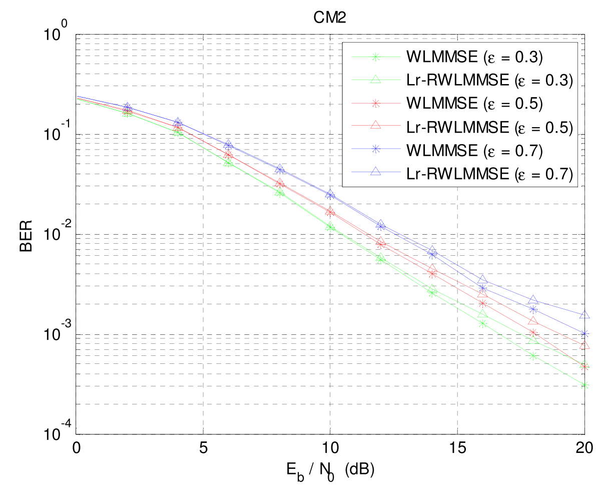

Figure 7 BER vs. SNR of WLMMSE and Lr-RWLMMSE estimators for ε∈{0.3, 0.5, 0.7} over CM2 channel model. BER, bit error rate; WLMMSE, widely linear minimum mean square error; Lr-RWLMMSE, low-rank real-valued widely linear minimum mean square error.

WLMMSE estimator's performance at high SNR. For Lr-RWLMMSE estimator, the performance degrades slightly as the rank r decreases. This is due to the loss of channel information when the rank of the channel correlation matrix is reduced. These results are further proved by the Figures 6 and 7 which give the performance of the WLMMSE and Lr-RWLMMSE with rank $r = 32$ for different values of rhombic deformation coefficient.

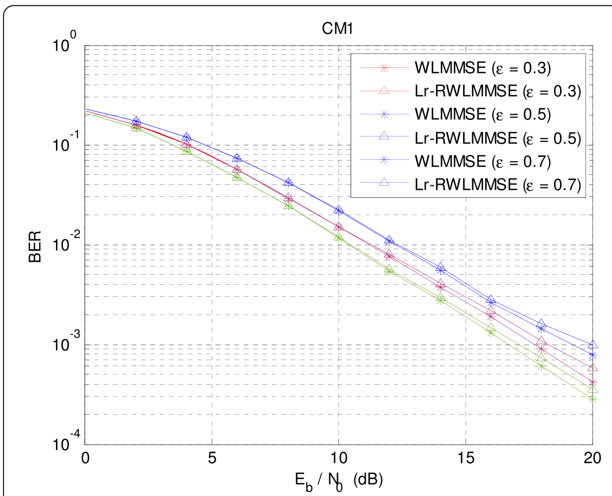

Figure 6 BER vs. SNR of WLMMSE and Lr-RWLMMSE estimators for ε∈{0.3, 0.5, 0.7} over CM1 channel model. BER, bit error rate; WLMMSE, widely linear minimum mean square error; Lr-RWLMMSE, low-rank real-valued widely linear minimum mean square error.

6 Conclusions

In this paper, we have presented a low-complexity channel estimator for MB-OFDM UWB system. We have investigated the WLMMSE channel estimator algorithm, and we have proceeded with real-valued algorithm followed by low-rank approximation of such channel estimator algorithm. The proposed low-rank real-valued WLMMSE channel estimator algorithm has reduced the computational complexity while maintaining the performance improvement of the WLMMSE one. As a consequence, the proposed Lr-RWLMMSE channel estimator algorithm has provided not only BER performance improvement but also lower computation cost.

Abbreviations

AWGN: additive white Gaussian noise; BER: bit error rate; CDMA: code division multiple access; CES: channel estimation sequence; DAC: digital-to-analog converter; DCM: dual carrier modulation; DS: direct sequence; DS-UWB: direct sequence ultra-wideband; EVD: eigenvalue decomposition; FCC: Federal Communications Commission; IFFT: inverse fast Fourier transform; LOS: line of sight; Lr: low rank; LS: least square; MAI: multiple-access interference; MB: multiband; MBOA: Multiband OFDM Alliance; MC: multi-carrier; MIMO: multiple input multiple output; MMSE: minimum mean square error; MSE: mean square error; NBI: narrowband interference; NLMS: normalized least mean square; NLOS: non-line of sight; OFDM: orthogonal frequency division multiplexing; OLA: over-lap-added; PLCP: physical layer convergence protocol; PPDU: PLCP protocol data unit; PSDU: PLCP service data unit; RR: reduced-rank; RRMLE: reduced-rank maximum likelihood estimation; RWLMMSE: real-valued WLMMSE; SER: signal error rate; SNR: signal-to-noise ratio; SVD: singular value decomposition; UWB: ultra-wideband; WF: Wiener filtering; WL: widely linear; WPAN: wireless personal area networks.

Competing interests

The authors declare that they have no competing interests.

Author details
[1]National Engineering School of Tunis/Innov'COM Lab, University of El-Manar, El Manar 1, 1068 Tunis, Tunisia. [2]National Engineering School of Sousse/SOIE, University of Sousse, B.P 264 Cité Erriadh, 4023 Sousse, Tunisia. [3]Sup'Com/Innov'COM Lab, Carthage University, Route de Raoued Km 3,5 El Ghazala, 2083 Ariana, Tunisia.

Received: 15 December 2014 Accepted: 10 February 2015
Published online: 10 March 2015

References

1. J Foerster, E Green, S Somayazulu, D Leeper, Ultra-wideband technology for short- or medium-range wireless communications. Intel Technology J Q2. (2001)http://www.intel.com/content/dam/www/public/us/en/documents/research/2001-vol05-iss-2-intel-technology-journal.pdf
2. A Batra, J Balakrishnan, GR Aiello, JR Foerster, A Dabak, Design of a multiband OFDM system for realistic UWB channel environments. IEEE Trans Microwave Theory Tech A **52**, 2123–2138 (2004)
3. A Batra, J Balakrishnan, A Dabak, R Gharpurey, J Lin, P Fontaine, JM Ho, S Lee, M Frechette, S March, H Yamaguchi, J Cheah, K Boehlke, J Ellis, N Askar, S Lin, D Furuno, D Peters, G Rogerson, M Walker, F Chin, Madhukumar, X Peng, Sivanand, J Foerster, V Somayazulu, S Roy, E Green, K Tinsley, C Brabenac et al., *Multi-Band OFDM Physical Layer Proposal for IEEE 802.15 Task Group 3a,* IEEE P802.15-03/268r3 (March 2004).
4. Standard ECMA-368, High rate ultra wideband PHY and MAC standard, 1st edition, Dec. 2005, 2nd edition, Dec. 2007, http://www.ecma-international.org/publications/standards/Ecma-368-arch.htm
5. T Jacobs, Y Li, H Minn, RMAP Rajatheva, Synchronization in MB-OFDM-Based UWB Systems*, Proceedings of the IEEE International Conference on Communications* (IEEE Xplore Press, 2007), pp. 1071–1076. doi:10.1109/ICC.2007.182
6. C Bairu, J Liangcheng, Synchronization Design for MB-OFDM Ultra Wideband (UWB) System, *Proceedings of the IEEE 13th International Conference on Communication Technology* (IEEE Xplore Press, 2011), pp. 485–488. doi:10.1109/ICCT.2011.6157923
7. Y Zhenzhen, C Duan, P Orlik, Z Jinyun, A Low-Complexity Synchronization Design for MB-OFDM Ultra-Wideband Systems*, Proceedings of the IEEE International Conference on Communications* (IEEE Xplore Press, 2008), pp. 3807–3813. doi:10.1109/ICC.2008.715
8. JJ Beek, O Edfors, M Sandell, SK Wilson, PO Borjesson, On Channel Estimation in OFDM Systems, Proceedings of the IEEE 45th Vehicular Technology Conference vol. 2 (IEEE Xplore Press, 1995), pp. 815–819. doi:10.1109/VETEC.1995.504981
9. Y Li, H Minn, RMAP Rajatheva, Synchronization, channel estimation, and equalization in MB-OFDM systems. IEEE Trans Wirel Commun **7**(11), 4341–4352 (2008)
10. S Coleri, M Ergen, Puri A, Bahai A, A study of channel estimation in OFDM systems*, Proceedings of the IEEE 56th Vehicular Technology Conference* (IEEE Xplore Press, 2002), pp. 894–898. doi:10.1109/VETECF.2002.1040729
11. SMR Islam, SK Kyung, Energy-Efficient Channel Estimation for MB-OFDM UWB System in Presence of Interferences, *Proceedings of the International Conference on Information and Communication Technology Convergence* (IEEE Xplore Press, 2010), pp. 149–154. doi:10.1109/ICTC.2010.5674256
12. T Ballal, TY Al-Naffouri, Low-sampling-rate ultra-wideband channel estimation using equivalent-time sampling. IEEE Trans Signal Process **62**(18), 4882–4895 (2014)
13. M Hajjaj, F Mhiri, R Bouallegue, Low-Complexity MMSE Channel Estimator for MB-OFDM UWB Systems. Int J Future Comp Communication A **3**, 227–231 (2014)
14. M Basaran, S Erküçük, HA Cirpan, Compressive sensing for ultra-wideband channel estimation: on the sparsity assumption of ultra-wideband channels. Int J Communication Systems (2013); [Online]. Available: http://dx.doi.org/10.1002/dac.2548.
15. P Hammarberg, F Rusek, O Edfors, Channel estimation algorithms for OFDM-IDMA: complexity and performance. IEEE Trans. Wirel. Commun. **11**(5), 1723–1734 (2012)
16. S Galih, T Adiono, A Kurniawan, Low complexity MMSE channel estimation by weight matrix elements sampling for downlink OFDMA mobile WiMAX system. Int J Computer Science and Network Security **10**(2), 280–285 (2010)
17. A Zaier, R Bouallegue, Channel estimation study for block - pilot insertion in OFDM systems under slowly time varying conditions. Int J Computer Networks & Communications (IJCNC) **3**(6), 39–54 (2011)
18. SMR Islam, KS Kwak, Preamble-based improved channel estimation for multiband UWB system in presence of interferences. Telecommunication Systems, doi:10.1007/s11235-011-9440-5. Published Online: 09 April 2011.
19. B Picinbono, P Chevalier, Widely linear estimation with complex data. IEEE Trans Signal Process **A43**, 2030–2033 (1995)
20. P Chevalier, JP Delmas, A Oukac, Properties, performance and practical interest of the widely linear MMSE beamformer for nonrectilinear signals. Signal Process A **97**, 269–281 (2014)
21. F Sterle, Widely linear MMSE transceivers for MIMO channels. IEEE Trans Signal Process A **55**, 4258–4270 (2007)
22. Y Cheng, M Haardt, *Widely Linear Processing in MIMO FBMC/OQAM Systems* (Proceedings of the ISWCS, Ilmenau, Germany, 2013)
23. S Abdallah, IN Psaromiligkos, Widely Linear Minimum Variance Channel Estimation for MC-CDMA Systems Using Real Modulation, *Proceedings of the Canadian Conference on Electrical and Computer Engineering* (IEEE Xplore Press, 2007), pp. 757–760. doi:10.1109/CCECE.2007.194
24. N Song, RC Lamare, M Haardt, M Wolf, Adaptive widely linear reduced-rank interference suppression based on the multistage wiener filter. IEEE Trans Signal Process **60**(8), 4003–4016 (2012)
25. J Szurley, A Bertrand, M Moonen, On the use of time-domain widely linear filtering for binaural speech enhancement. IEEE Signal Processing Letters A **20**, 649–652 (2013)
26. FGA Neto, VH Nascimento, MTM Silva, Reduced-Complexity Widely Linear Adaptive Estimation, *Proceedings of* the *7th International Symposium on Wireless Communication Systems* (IEEE Xplore Press, 2010), pp. 399–403. doi:10.1109/ISWCS.2010.5624294
27. P Stoica, M Viberg, Maximum likelihood parameter and rank estimation n reduced-rank multivariate linear regressions. IEEE Trans Signal Processing A **44**, 3069–3078 (1996)
28. LL Scharf, B Van, Veen, Low rank detectors for Gaussian random vectors. IEEE Transactions on Acoustics Speech and Signal Processing A **35**, 1579–1582 (1987)
29. RC de Lamare, R Sampaio-Neto, Reduced-rank adaptive filtering based on joint iterative optimization of adaptive filters. IEEE Signal Processing Letters **14**(12), 980–983 (2007)
30. A Marzook, A Ismail, A Sali, BM Ali, S Khatun, A new technique for multi-cell joint channel estimation in time division code division multiple access based on reduced rank singular value decomposition. Springer Wireless Networks **20**(4), 759–773 (2014)
31. AM Haimovich, Y Bar-Ness, An eigen analysis interference canceler. IEEE Trans on Signal Processing **A 39**, 76–84 (1991)
32. Y Hua, M Nikpour, P Stoica, Optimal reduced rank estimation and filtering. IEEE Trans Signal Process **49**(3), 457–469 (2001)
33. JS Goldstein, IS Reed, LL Scharf, A multistage representation of the Wiener filter based on orthogonal projections. IEEE Trans Inf Theory **A44**, 2943–2959 (1998)
34. ML Honig, JS Goldstein, Adaptive reduced-rank interference suppression based on the multistage Wiener filter. IEEE Trans On Communications **50**(6), 986–994 (2002)
35. O Edfors, M Sandell, JJ van de Beek, SK Wilson, PO Börjesson, OFDM channel estimation by singular value decomposition. IEEE Trans Commun **46**(7), 931–939 (1998). doi:10.1109/26.701321
36. T Cui, Q Wang, Y Jing, X Yu, SVD-Based Estimation for Reduced-Rank MIMO Channel, *Proceedings of the IEEE International Symposium on Information Theory* (IEEE Xplore Press, 2014), pp. 631–635. doi:10.1109/ISIT.2014.6874909
37. RC de Lamare, R Sampaio-Neto, Adaptive reduced-rank processing based on joint and iterative interpolation, decimation, and filtering. IEEE Trans Signal Process **57**(7), 2503–2514 (2009)
38. S Li, RC de Lamare, R Fa, Reduced-Rank Linear Interference Suppression for DS-UWB Systems Based on Switched Approximations of Adaptive Basis Functions. IEEE Trans Veh Technol **60**(2), 485,497 (2011)
39. Z Sahinoglu, S Gezici, I Guvenc, *Ultra-Wideband Positioning Systems: Theoretical Limits, Ranging Algorithms, and Protocols* (Cambridge University Press, New York, 2008)
40. J Foerster (editor), *Channel Modeling Sub-Committer Report Final* (tech. rep., IEEE P802, IEEE P802.15 Working Group for Wireless Personal Area Networks, 2004). 15-02/368r5-SG3a

41. B Muquet, Z Wang, GB Giannakis, M de Courville, P Duhamel, Cyclic prefixing or zero padding for wireless multicarrier transmissions? IEEE Trans Commun **50**(12), 2136–2148 (2002)
42. RM Gray, LD Davisson, *An Introduction to Statistical Signal Processing* (Cambridge Univ. Press, Cambridge, UK, 2004)
43. AT Fam, Efficient complex matrix multiplication. IEEE Trans Comput **37**(7), 877–879 (1988)